

*Original Scientific Article***MORPHOMETRIC AND HISTOCHEMICAL FEATURES OF THE HARDERIAN GLAND IN RABBITS WITH DIFFERENT TYPES OF AUTONOMOUS REGULATION**Andrii Tybinka¹, Marta Zakrevska², Olga Shchebentovska¹

¹*Department of Normal and Pathological Morphology and Forensic Veterinary Medicine, Stepan Gzhytskyi National University of Veterinary Medicine and Biotechnologies Lviv, 50 Pekarska St., 79010 Lviv, Ukraine*

²*Doctor Markevych's Veterinary Clinic, 2a Lysenytska Str., 79032 Lviv, Ukraine*

Received 28 January 2022; Received in revised form 11 May 2022; Accepted 5 August 2022

ABSTRACT

The tonus of autonomous centers reflected in the morpho-functional features of the organs in mammals. The study aimed to establish the influence of the autonomous regulation and its' typological peculiarities on the structural features of the rabbits' Harderian gland. Clinically healthy male rabbits, four months old, weighing 3.6-3.9 kg, were selected for the research. Based on the study of heart rate variability, three types of autonomous regulation were outlined, according to which three groups of rabbits were formed: ST rabbits (sympathetic dominant regulation), PS rabbits (parasympathetic dominant regulation), and NT rabbits (combined sympathetic and parasympathetic regulation). After euthanasia, the Harderian gland was dissected in all animals. Histological specimens were prepared and a morphometric examination was performed. ST rabbits corresponded to the minimal indicators in the tubular alveoli in both parts of the gland, as well as the maximum indicators of capsule thickness. NT rabbits corresponded to the maximum values of the acini area in the pink lobe, and in the white lobe - the maximal values of the cross-sectional area of the tubular alveoli, its wall area, and the epithelium height. The maximum acini area corresponded to PS rabbits in the white lobe, and in the pink lobe - the maximum indicators of the tubular alveoli cross-sectional area, and epithelial height. The pink and white lobes' structure of the rabbit's Harderian gland was affected by the combined tonus of the sympathetic and parasympathetic centers. The findings elucidate the regulatory and trophic effects on the Harderian gland in rabbits.

Key words: Harderian gland, rabbits, tubular alveoli, morphometry, autonomous regulation

INTRODUCTION

The Harderian gland is a multifunctional organ in mammals that secretes lipids, porphyrins, pheromones, and promotes photoreception and hormone secretion (1, 2). In birds, the gland performs a pronounced immune function (3, 4, 5). Morpho-functional characteristics of the Harderian

gland depend on the organism's functional state (6), circadian (7), and seasonal (8) rhythms.

Among mammals, the Harderian gland is best developed in rodents and hares (9, 10). The gland consists of larger and smaller lobes. The lobes differ by color only in rabbits: the smaller part is white, while the larger is pink. Each lobe is divided into smaller parts (acini), separated by layers of connective tissue, and has tubular alveoli. The gland has a single excretory duct that terminates on the surface of the third eyelid (9).

The pink and white lobes' tubular alveoli wall is formed by a single layer of glandular epithelium on the basement membrane. In most animals, including rats (11), guinea pigs (12), and hamsters (13), the epithelium of both lobes has the same structure and consists of two or three (rarely four) cell types at the same time. However, regarding rabbits, the epithelium of each lobe differs and is represented

Corresponding author: Prof. Andrii Tybinka, PhD

E-mail address: a.m.tybinka@gmail.com

Present address: Department of Normal and Pathological Morphology and Forensic Veterinary Medicine, Stepan Gzhytskyi National University of Veterinary Medicine and Biotechnologies Lviv, 50 Pekarska St., 79010 Lviv, Ukraine
Phone: +380673530320

Copyright: © 2022 Tybinka A. This is an open-access article published under the terms of the Creative Commons Attribution License which permits unrestricted use, distribution, and reproduction in any medium, provided the original author and source are credited.

Competing Interests: The authors have declared that no competing interests exist.

Available Online First: 31 August 2022

Published on: 15 October 2022

<https://doi.org/10.2478/macvetrev-2022-0024>

by only one specific type of epitheliocytes, which in the pink lobe are mostly cubic and contain large lipid vacuoles. In the white lobe, the vacuoles' size is twice smaller, and the epitheliocytes are mostly columnar (14).

A mixed lobe is sometimes found at the junction point of the pink and white lobes. It combines tubular alveoli from previous lobes and tubular alveoli that simultaneously contain different types of epitheliocytes (15).

Parasympathetic fibers enter the gland through the facial nerve (16), while sympathetic fibers enter along the arteries from the upper cervical ganglion (17). It has been established (18) that the autonomous regulation peculiarities affect the structure of the rabbits' adrenal gland. Therefore, this study aimed to determine the relationship between the Harderian gland's morphology and the autonomous regulation type in rabbits.

MATERIAL AND METHODS

Experimental animals

Clinically healthy male rabbits (*Oryctolagus cuniculus*) of the Blanc de Termonde breed, four months old, weighing 3.6-3.9 kg, were obtained from a local farm.

Study of autonomous regulation (AR)

Peculiarities of autonomous regulation were defined based on the electrocardiographic study of heart rate variability (19). A rheograph P4-02 (PEMA, Ukraine) with an electrocardiographic channel and a recording device H338-6P (PEMA, Ukraine) were used for this purpose. The tape drawing speed when recording the cardio signal was 250 mm/s. The geometric method of estimating the intervals R-R (20) was applied to analyze the electrocardiograms based on the definition of the following indicators: mode (Mo) - the value of the R-R interval, which occurred most often; mode amplitude (AMo) - the number of R-R intervals that form the mode (expressed in %); variation range (MxDMn) - the difference between the longest (Mx) and the shortest (Mn) R-R intervals.

Based on the obtained results, three types of autonomous regulation were established, according to which three groups of rabbits (five animals each) were formed:

1) ST rabbits - characterized by the dominance of the sympathetic centers' tonus (Mo \leq 1.25 s; AMo \geq 21%; MxDMn \leq 10 s);

2) PS rabbits - characterized by the dominance of the parasympathetic centers' tonus (Mo: \geq 1.41 s; AMo: \leq 15%; MxDMn \geq 36 s);

3) NT rabbits - characterized by the balanced tonus of sympathetic and parasympathetic centers (Mo: 1.26-1.40 s; AMo: 16-20%; MxDMn 11-35 s).

Ethical approval

Ethical standards for animals used in experiments were followed during the research (Directive 2010/63/EU, 2010 (21)). The research methodology was approved by the Ethics Commission of the Lviv National University of Veterinary Medicine and Biotechnology named after S. Gzhytskyi (protocol №5 dated 26.10.2016). Euthanasia of the animals was performed by overdose inhalation of chloroform.

Histological, histochemical, and morphometric study

The prepared Harderian gland was divided into fragments and fixed in Bouin's solution for 24 hours, washed for 24 hours in 70% ethanol, dehydrated in increasing ethanol concentration (70-96%), clarified in xylene, and placed in paraffin blocks. Using the MS-2 sled microtome (TOCHMEDPRYBOR, Ukraine), 7- μ m-thick sections were prepared from the blocks, and consequently placed on glass, dried, dewaxed in xylene, rehydrated (in the lowering ethanol concentration (96-70%)), painted and then, the slides were covered using Canada balsam resin and coverslip (22). To study the gland's general structure, sections were stained (22) with Mayer's hematoxylin and eosin, collagen fibers were detected by the Heidenhain's azan staining, and elastic fibers were revealed by Weigert's resorcin-fuchsin staining. Histochemical reactions (23) were also used to detect neutral mucosubstances (Periodic Acid Schiff (PAS)) and acidic mucosubstances (Alcian blue, pH 2.5 (AB)).

Histological examination and photo fixation by photomicrographs were performed using a Leica DM-2500 light microscope with a Leica DFC450C camera and Leica Application Suite 4.4 software (Leica Microsystems GmbH, Germany). Aperio Image Scope software (Leica Biosystems, USA) was used for the morphometric study. The number of collagen fibers, elastic fibers, and PAS-positive structures was analyzed by determining their optical density using the WCIF ImageJ software (WCIF, Canada).

The relative area in % of the tubular alveolus's wall was determined according to the following equation:

$$(A/B) \times 100 = \%,$$

where, A is the absolute area (μm^2) of the tubular alveolus's wall; and B is the absolute cross-sectional area of the entire tubular alveolus (μm^2).

Statistical analysis

Statistical analysis of the results was performed using the one-way ANOVA, taking into account the Bonferroni correction. The calculations were done using StatPlus software (AnalystSoft Inc., USA). It was also used for Pearson correlation analysis. The results are presented as Mean \pm SD. The differences between the animal groups were considered statistically significant at $p < 0.05$. At the same time, statistical analysis of indicators was carried out separately for the pink and white lobes.

RESULTS

The acini into which the gland's pink and white lobes were divided had various shapes. Most of them were elongated and oval (Fig. 1). There were round, triangular, rectangular, and irregularly shaped acini, as well. The influence of the

autonomous regulation typological peculiarities on this feature was not revealed. However, this effect was detected in the acini size (Table 1).

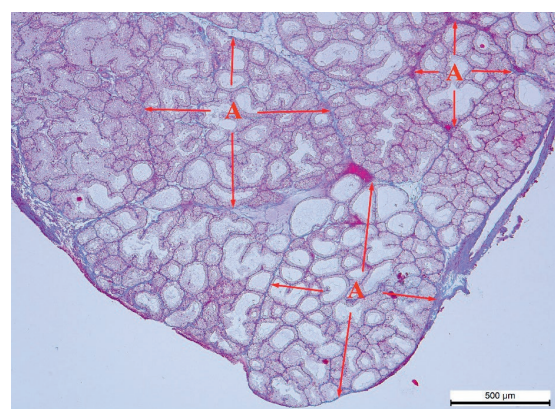


Figure 1. Connective tissue (blue color), which limits the acini (A and red arrows) in the pink lobe of the NT rabbit's Harderian gland. Heidenhain's azan staining. Magnification: $\times 50$. Scale bar = $500 \mu\text{m}$

The smallest acini were found both in pink ($1.56 \pm 0.18 \text{ mm}^2$) and white ($0.89 \pm 0.28 \text{ mm}^2$) lobes in ST rabbits. The maximum acini area was almost the same, however, in the pink lobe ($2.32 \pm 0.66 \text{ mm}^2$) it corresponded to NT rabbits while in the white lobe ($2.34 \pm 0.25 \text{ mm}^2$) the area corresponded to PS rabbits.

Table 1. Morphometric indicators of the rabbit's Harderian gland

Indicator	AR type	Gland's lobe	
		Pink	White
Acinus area, mm^2	ST	1.56 ± 0.18	0.89 ± 0.28
	NT	2.32 ± 0.66	1.44 ± 0.22^a
	PS	1.77 ± 0.23	2.34 ± 0.25^{bc}
Tubular alveolus's cross-sectional area, μm^2	ST	10755.07 ± 892.42	10290.49 ± 642.94
	NT	12871.09 ± 1215.77	12527.20 ± 2043.70
	PS	13397.63 ± 795.40^b	12414.62 ± 512.28^b
Tubular alveolus's lumen area, μm^2	ST	6717.99 ± 624.48	5432.33 ± 537.20
	NT	7367.81 ± 1091.57	6026.27 ± 1054.03
	PS	6980.53 ± 519.36	6215.39 ± 469.39
Tubular alveolus's wall area, μm^2	ST	4037.08 ± 495.96	4858.15 ± 208.37
	NT	5503.28 ± 846.96^a	6500.92 ± 1289.61
	PS	6417.10 ± 280.06^{bc}	6199.23 ± 81.94^b
Tubular alveolus's relative wall area, %	ST	37.54 ± 3.29	47.21 ± 2.39
	NT	42.76 ± 5.49	51.89 ± 4.62
	PS	47.90 ± 0.82^{bc}	49.93 ± 1.77
Tubular alveolus's epithelium height, μm	ST	13.40 ± 1.12	15.44 ± 0.69
	NT	13.92 ± 1.07	18.19 ± 1.16^a
	PS	17.60 ± 0.54^{bc}	14.98 ± 1.03^c

AR – autonomous regulation; a - statistically significant difference between NT and ST groups (a - $p < 0.05$); b - statistically significant difference between PS and ST groups (b - $p < 0.05$); c - statistically significant difference between PS and NT groups (c - $p < 0.05$)

In all types of autonomous regulation, the average cross-sectional area of the pink lobe's tubular alveoli was larger than that of the white (Fig. 2). At the same time, in both lobes, the smallest indicators of the area corresponded to ST rabbits. The indicators were significantly higher in PS animals.

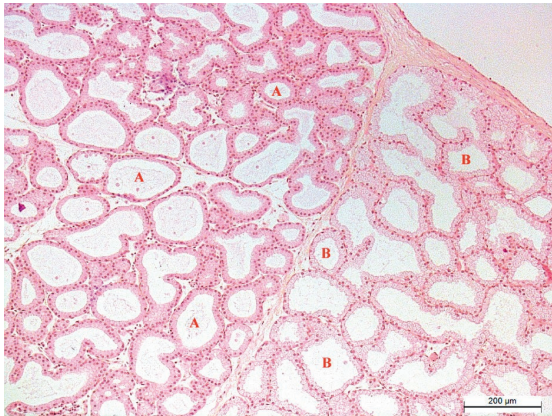


Figure 2. Tubular alveoli of the white (A) and pink (B) lobes of the ST rabbit's Harderian gland. Hematoxyline and eosin staining. Magnification: $\times 100$. Scale bar=200 μm

The tubular alveoli cross-sectional area consisted of the lumen area and the wall area formed by the epithelial cells. The relationship between them depended both on the type of autonomous regulation and the gland proportion. The lowest values of both indicators corresponded to the ST rabbits again. The lumen area in the white lobe was smaller than in the pink. As for the wall area (μm^2), the complete dominance of one lobe over

another was not detected according to the absolute indicators. There was a significant increase of this indicator in the pink lobe when parasympathetic tonus (PS) predominates, and in the white lobe - under balanced tonus of the sympathetic and parasympathetic centers (NT). At the same time, the relative wall area in the white lobe exceeded that of the pink lobe by 9.67% in ST rabbits, 9.13% in NT rabbits, and 2.03% in PS rabbits. It should be noted that only in the white lobe of NT animals does the wall area amount to more than half (51.89%) of the tubular alveoli' total area. The figure did not reach 50% in all other cases. The tubular alveoli lumen area, in contrast to their wall area, did not differ significantly in the studied groups of rabbits.

Epithelial cells in pink and white lobes differed both in height and shape. The height of epitheliocytes did not depend on the tubular alveoli size. However, it was associated with the typological features of autonomous regulation. The lowest epithelial layer was found in the pink lobe of the ST rabbits and in the white lobe of the PS rabbits. PS and NT rabbits had the highest values for this indicator. In this case, the difference between these groups was 4.20 μm ($p < 0.05$) in the pink lobe and 3.21 μm ($p < 0.05$) in the white lobe.

Most of the tubular alveoli within the pink (Fig. 3A) and white (Fig. 3B) lobes contained epitheliocytes of the same shape, i.e. cubic and columnar.

However, the cubic epitheliocytes were combined with the flat ones in a number of the pink lobe's tubular alveoli (Fig. 4A). The columnar epitheliocytes were combined with the cubic and flat types in the white lobe (Fig. 4B). The cells of the last two groups also formed independently the

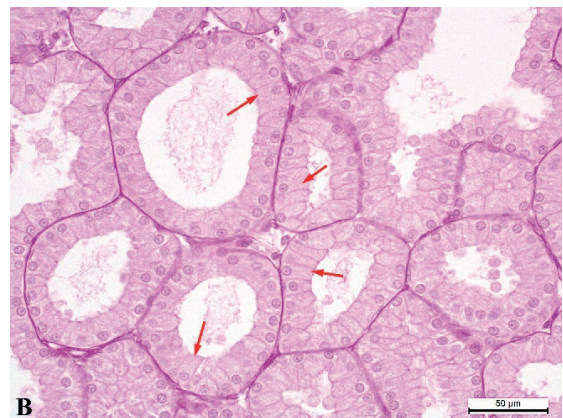
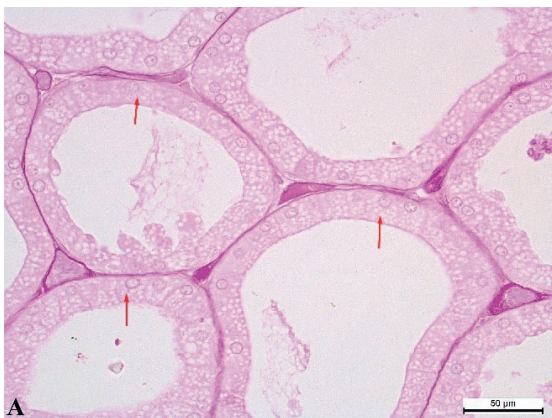


Figure 3. Tubular alveoli of the PS rabbit's Harderian gland: pink lobe - cubic epitheliocytes (red arrows) (A); white lobe - columnar epitheliocytes (red arrows) (B). PAS reaction. Magnification: $\times 400$. Scale bar=50 μm

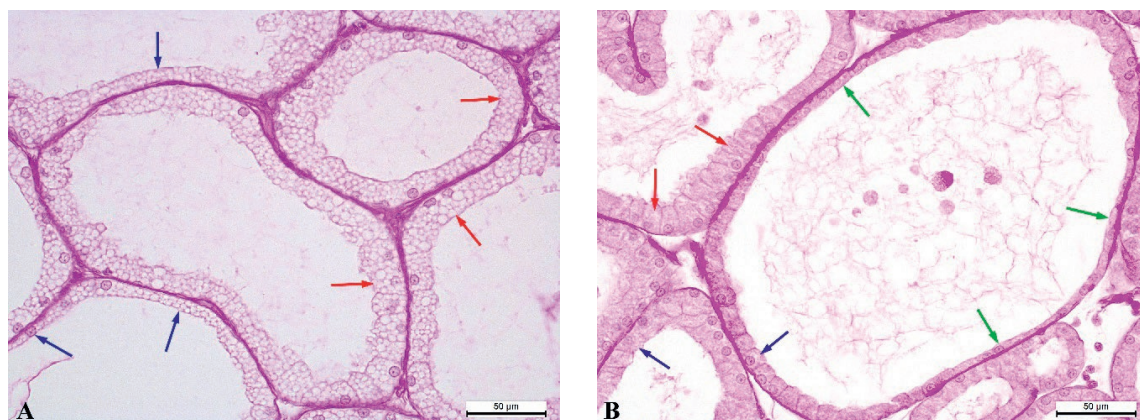


Figure 4. Tubular alveoli of the PS rabbit's Harderian gland: pink lobe - cubic epitheliocytes (red arrows) and flat epitheliocytes (blue arrows) (A); white lobe - columnar epitheliocytes (red arrows), cubic epitheliocytes (blue arrows), flat epitheliocytes (green arrows) (B). PAS reaction. Magnification: $\times 400$. Scale bar=50 μm

epithelial layer of individual tubular alveoli. This was most characteristic for the large tubular alveoli. At the same time, in some areas of the gland, tubular alveoli with different epithelial heights were located in mixed order but formed separate groups in the other areas. These features were observed in all types of autonomous regulation.

According to the correlation analysis results, it was found out that the acinus area of the NT rabbits' pink lobe has a high positive correlation with the cross-sectional area of the tubular alveoli ($r=0.91$), its wall area ($r=0.77$), and its epithelium height ($r=0.80$). In the white lobe, the acinus area has a high positive correlation with the cross-sectional area of the tubular alveoli in NT animals ($r=0.68$), PS ($r=0.80$), and a medium negative correlation in ST rabbits ($r=-0.53$). The acinus area has a high

negative correlation with the epithelium height of the tubular alveoli in ST animals ($r=-0.87$), and NT animals ($r=-0.95$).

The gland capsule was characterized by significant variations in thickness and morphology. Capsule thickness (Table 2) had the greatest variability among all studied indicators. At the same time, the variation coefficient reached 46.14% in NT rabbits' white lobe and 49.75% in ST rabbits' pink lobe. In both lobes, the capsule thickness was characterized by close values and similar distribution of indicators between the autonomous regulation types. The thinnest capsule was found in PS rabbits, intermediate values were observed in NT rabbits, and ST animals had the maximum values. Generally, the capsule was thicker in the area of the pink lobe than in the area of the white lobe in all groups.

Table 2. Stroma morphometric parameters of the rabbits' Harderian gland

Indicator	AR type	Gland's lobe	
		Pink	White
Capsule thickness, μm	ST	27.99 \pm 13.93	26.03 \pm 10.70
	NT	22.10 \pm 6.43	21.30 \pm 9.83
	PS	19.86 \pm 3.86	19.29 \pm 5.48
Proportion of capsule occupied by collagen fibers, %	ST	72.28 \pm 6.71	71.48 \pm 4.19
	NT	63.31 \pm 8.76	67.77 \pm 4.69
	PS	71.21 \pm 2.91	62.81 \pm 2.35 ^b
Share of interalveolar space occupied by collagen fibers,%	ST	3.96 \pm 0.48	3.43 \pm 0.51
	NT	2.17 \pm 0.16 ^a	2.01 \pm 0.27 ^a
	PS	3.46 \pm 0.22 ^c	3.32 \pm 0.19 ^c
Share of PAS-positive structures in the tubular alveoli area, %	ST	4.51 \pm 0.50	6.78 \pm 0.56
	NT	5.33 \pm 0.52	7.09 \pm 0.22
	PS	5.65 \pm 0.31 ^b	6.68 \pm 0.38

AR – autonomous regulation; a - statistically significant difference between NT and ST groups (a - $p < 0.05$); b - statistically significant difference between PS and ST groups (b - $p < 0.05$); c - statistically significant difference between PS and NT groups (c - $p < 0.05$)

Collagen fibers formed the capsule's structural basis (Fig. 5). There was a decrease in the number of collagen fibers (%) in the capsule of the white lobe in the rabbits with dominant parasympathetic tonus (PS). In the pink part of the gland, this process was observed under the balanced tonus of the sympathetic and parasympathetic centers (NT). The maximum saturation of collagen fibers in the pink ($72.28 \pm 6.71\%$) and white ($71.48 \pm 4.19\%$) lobes was also similar, but occurred in animals of the dominant autonomous regulation type, i.e. ST rabbits.

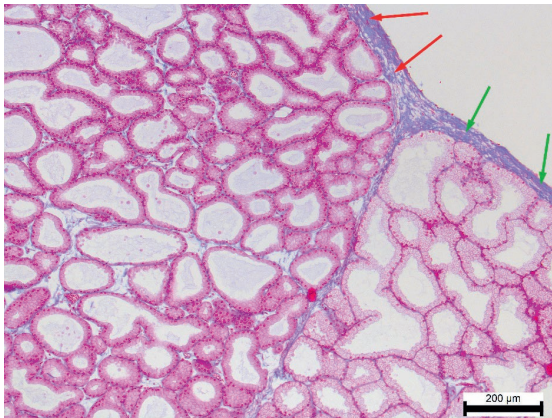


Figure 5. Collagen fibers (blue color) in the capsule of the white lobe (red arrows) and pink lobe (green arrows) of the ST rabbit's Harderian gland. Heidenhain's azan staining. Magnification: $\times 100$. Scale bar=200 μm

A small number of collagen fibers was also found in the tubular alveoli basement membranes and the connective tissue layers between them (Fig.

6). Their relationship to the autonomous regulation type was similar to the one of the gland capsule. In other words, higher rates in both lobes were observed in the ST rabbits. NT rabbits, on the contrary, demonstrated a minimal amount of collagen fibers. The difference between them was as follows: in the pink lobe - 1.79% ($p < 0.05$), in the white lobe - 1.42% ($p < 0.05$).

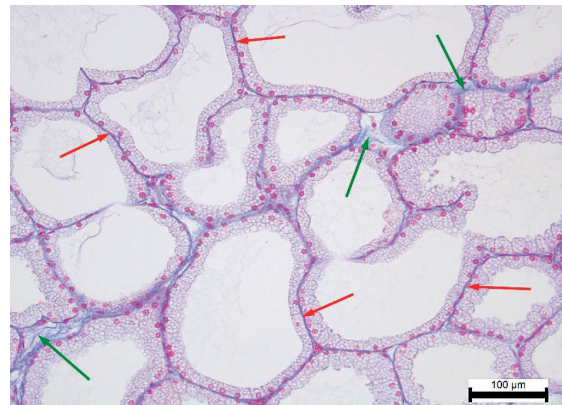


Figure 6. Collagen fibers (blue color) in the basement membranes of the tubular alveoli (red arrows) and in the connective tissue layers between them (green arrows) in the pink lobe of the NT rabbit's Harderian gland. Heidenhain's azan staining. Magnification: $\times 200$. Scale bar=100 μm

The elastic fibers' location in the gland capsule did not have a pronounced pattern and had high quantitative variability (Fig. 7). Thus, the area with a relatively thick capsule, completely devoid of elastic fibers, passed into an area with the capsule

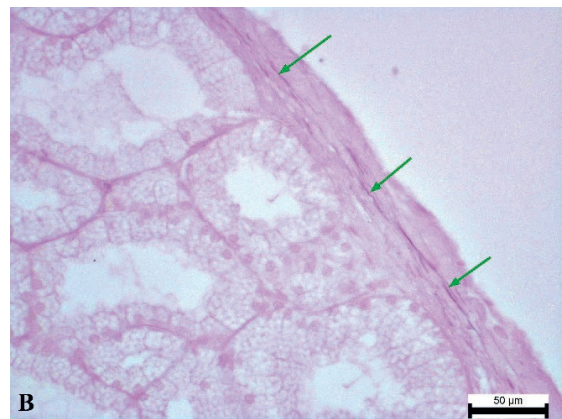
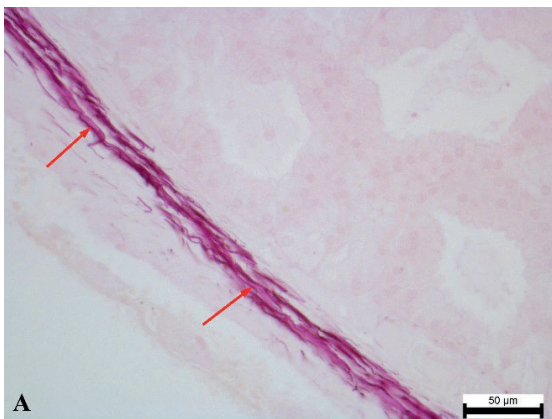


Figure 7. the white lobe's capsule of the ST rabbit's Harderian gland with a high content of elastic fibers (red arrows) (A); the pink lobe's capsule of the ST rabbit's Harderian gland with a low content of elastic fibers (green arrows) (B). Weigert's resorcin-fuchsin staining. Magnification: $\times 400$. Scale bar=50 μm

twice as thin, which contained a dense network of elastic fibers. There were also areas containing thin and single elastic fibers. The regularities of this process weren't identified. Therefore, the morphometric study of the existing fibers was performed, without static processing of the results. It was found that the number of elastic fibers in ST and PS rabbits was approximately equal in both lobes of the gland, ranging from 5-6% to 16-17% of the capsule thickness. In NT animals, this figure was 16-25% in the pink lobe and ranged very significantly in the white lobe, i.e. from 7% to 69%.



Figure 8. White lobe's elastic fibers of the NT rabbit's Harderian gland: in the arterioles wall (red arrow), in the venules wall (blue arrow), in the excretory duct wall (green arrow). Weigert's resorcin-fuchsin staining. Magnification: $\times 200$. Scale bar=100 μm

The presence of elastic fibers in the connective tissue septa separating the gland lobes and acini largely depended on the abundance of these fibers in the capsule from which these septa began. The blood vessels' wall and the gland's excretory ducts, as well as the area around the nerve trunks, were stable places for the elastic fibers' localization (Fig. 8). Elastic fibers were not observed in more than 90% of the cases in the connective tissue layers between the tubular alveoli. Individual elastic fibers were sometimes found to penetrate between individual alveoli located either under the capsule or near the connective tissue septa.

PAS-positive substances were present in all parts of the Harderian gland. In this study, the PAS response was analyzed only in the tubular alveoli area, excluding gland capsules and areas of vascular, excretory ducts, and nerves. The epithelial cells' cytoplasm showed a weak PAS response. Instead, it was pronounced in the basement membrane and connective tissue of the interalveolar space (Fig. 9). In general, the relative area of structures with a strong PAS response in the pink lobe was smaller than in the white lobe.

The increase in the number (%) of PAS-positive structures in the pink lobe was observed under the predominance of parasympathetic tonus (PS), and in the white lobe - under balanced tonus of the sympathetic and parasympathetic centers (NT). The difference between the maximum and minimum indicators in these groups was 1.14% ($p < 0.05$) and 0.41%, respectively.

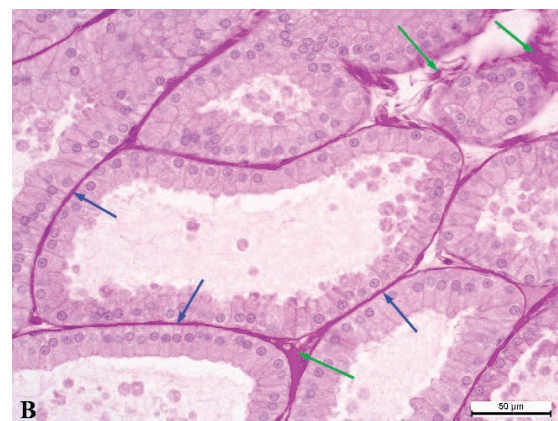
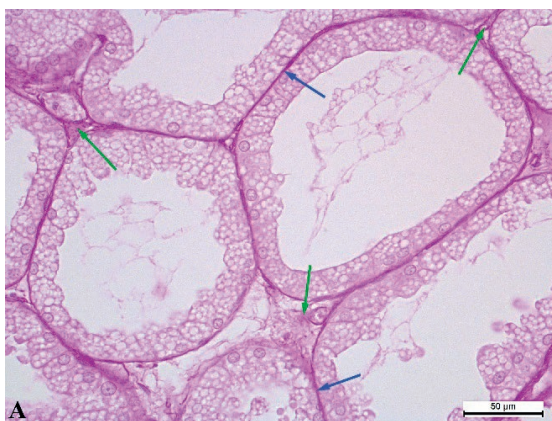


Figure 9. High concentration of PAS positive substances in the tubular alveoli' basement membranes (blue arrows) and in the connective tissue layers between them (green arrows) in the PS rabbit's Harderian gland: pink lobe (A); white lobe (B). PAS reaction. Magnification: $\times 400$. Scale bar=50 μm

Histochemical detection of acidic mucosubstances using Alcian blue (pH 2.5) did not yield results. The chemicals were not found in the structure of the rabbits' Harderian gland.

A mixed lobe was also found between the pink and white lobes of the gland. It has not been studied since the significant features of its structure require separate research.

Based on the correlation analysis, it was found that the cross-sectional area of the tubular alveoli has a high negative correlation with the number of PAS-positive structures of the interalveolar space in ST and PS animals. The cross-sectional area in the pink lobe was $r=-0.70$ and $r=-0.83$ respectively, and in the white lobe $r=-0.62$ and $r=-0.88$ respectively. In the white lobe, a similar type of correlation was found between the cross-sectional area of the tubular alveoli and the number of collagen fibers in the interalveolar space in the NT rabbits ($r=-0.93$) and PS rabbits ($r=-0.75$).

DISCUSSION

The presented study revealed that the combination peculiarities of sympathetic and parasympathetic centers' tonus form three types of autonomous regulation which affect the structure of the rabbits' Harderian gland due to their regulatory and trophic influences. Thus, a high level of sympathicotonia causes a decrease in the tubular alveoli size in both Harderian gland's lobes. At the same time, the average area of the pink lobe's tubular alveoli was larger than that of the white lobe under all types of autonomous regulation. This corresponds to the data obtained by other scientists (11), but the predominance of the pink lobe was significantly greater in their studies. This may be due to the breed features of the Harderian gland's morphology.

The availability of tubular alveoli with a different epithelial layer height reflects the gland's functional features within the pink and white lobes. The epithelial cells that were in the final stage of secrete accumulation mostly had the same height and shape with a relatively smooth apical surface. During the secretion phase, the surface had varying convexity and wavy conformation. After cessation of secretion, the apical surface of the epitheliocytes became smooth with decreased height changing the shape from columnar to cubic, and from cubic to flat. As a result, the tubular alveolus' wall area decreased and its lumen area increased. Then the epitheliocytes returned to the stage of

secretion accumulation again, and restored their size and shape, repeating the cycle. Therefore, the relationship between the wall area and the lumen area of the tubular alveoli allows for characterizing their functional state. The significant differences in the epitheliocytes height between the animal groups were correlated to the different type of autonomous regulation. The regulation of secretion by the autonomous nervous system has been previously studied by Di Matteo (24) without taking into account the different autonomic nervous patterns. The morpho-functional changes in epitheliocytes during secretion have also been described in the Harderian gland of hamsters (25), guinea pigs (26), and other animals (27).

Since different areas of the Harderian gland contain tubular alveoli with different epitheliocyte heights and shapes, it can be deduced that the secretion is not simultaneous. Based on our observations, this process can occur in three ways: a) individual tubular alveoli; b) groups of tubular alveoli; c) whole acini. Gradual secretion of individual tubular alveoli has also been described by Eltony (11).

Similar to the morphology of the tubular alveoli epithelial layer, the types of autonomous regulation were also manifested by the PAS response intensity of the same area. The strength of its expression in rabbits of the experimental groups was distributed according to the same pattern as the epitheliocytes height. The relationship between glandular function and PAS response has also been demonstrated in other animals (28, 29).

Although the capsule is a relatively passive part of the organ and does not provide its functional characteristics, it adapts to its structure (30). The morphological examination of the Harderian gland's capsule revealed a pronounced heterogeneity of its various areas, which, first of all, was manifested in significant fluctuations in thickness, both in the pink and white lobes. This is apparently due to the different functional features of the capsule's separate areas, some of which are adjacent to the bone orbit through the fascia, while others are in contact with the eye and its muscles. The orbital venous sinus, promoting the gland secretion, is adjacent to the Harderian gland's capsule (31). Significantly smaller fluctuations in capsule thickness were found in the Harderian gland of European bison (32) and ostrich (33).

The pronounced unevenness in the localization and number of elastic fibers was indicative that there were individual morpho-functional features in different parts of the Harderian gland capsule. To

our opinion, the number of elastic fibers increased in areas that were more stretched or stressed. It allowed for maintaining the optimal functional state of these areas. To some extent, this process depended on the autonomous regulation type, which determined the functional characteristics of the entire gland. The peculiarities of the elastic fibers' location in the Harderian gland capsule have also been studied in goats (34).

The capsule's collagen fibers had similar density in animals of different groups. This indicates a minor functional role and hence lower regulatory influences from the autonomous nervous system.

In general, the functions of elastic and collagen fibers as a part of the Harderian gland's extracellular matrix are similar to the other glands. These fibers perform a frame-protective function, maintain the integrity of the gland's structure during mechanical stresses during secretion, and adapt to the peculiarities of regulatory influences. In addition, the Harderian gland's connective tissue is also involved in the body's immune responses since it contains clusters of plasma cells (35).

Unlike rabbits, other mammals and birds contain acidic mucosubstances in the tubular alveoli of the gland (36, 37, 38). This indicates significant species-specific features in the Harderian gland's functioning.

It should also be noted that the ward gland is under the influence of endocrine glands despite the autonomic regulation. The pituitary gland (39), pineal gland (40), and gonads (41) regulate the gland's secretory activity. The thyroid gland maintains the structural integrity of the Harderian gland (42).

The obtained results are of clinical significance. They must be taken into account when studying the individual characteristics of the eye-protective mechanisms. The identified types of autonomic regulation may manifest themselves in the peculiarities of specific pathologies and the course of regenerative processes in this area. Differences in the gland's secretory activity (in particular, participation in the porphyrin synthesis), which may occur in the established groups of rabbits, reflect the functional state of the whole organism. However, this requires further research.

Considering the Harderian gland's autonomous regulation, future research should focus on the peculiarities of embryonic formation of its various types, as well as on the possible influence of environmental factors on this process.

CONCLUSION

Different types of autonomous regulation can affect the structure of the Harderian gland's pink and white lobes. The cross-sectional area of the pink lobe's tubular alveoli was larger than that of the white lobe regardless of the autonomous regulation type. The ST rabbits had the smallest acinus area in both lobes, whereas in the PS rabbits it was significantly higher. ST rabbits had the lowest epithelial layer in the pink lobe, whereas the PS rabbits had the lowest epithelial layer in the white lobe. The thickest epithelial layer was found in the PS and NT rabbits, respectively. The relative area of structures showing a strong PAS response in the pink lobe was smaller than in the white lobe. The lowest PAS-positive responses in ST rabbits were observed in the pink lobe whereas in the PS rabbits in the white lobe. Conversely, the highest PAS-positive area was observed in the pink lobe of the PS rabbits and the white lobe of the NT rabbits. The relationship between the wall area and the lumen area of tubular alveoli characterizes the functional state of the latter. No acidic mucosubstances were detected in the structure of the rabbit's ward gland.

CONFLICT OF INTEREST

The authors declared that they have no potential conflict of interest with respect to the authorship and/or publication of this article.

ACKNOWLEDGEMENTS

The study was supported by the Research Laboratory of the Department of Normal and Pathological Morphology and Forensic Veterinary Medicine and the Faculty of Veterinary Medicine in the National University of Veterinary Medicine and Biotechnologies named after Stepan Gzhytskyi, Lviv, Ukraine.

AUTHORS' CONTRIBUTION

AT developed the study's concept and methodology and participated in cardiographic research. MZ provided the research organization, histological specimens' production, their morphometric study, and statistical analysis of data. OS participated in data analysis and result interpretation. All authors participated in writing the article.

REFERENCES

1. Dunn, D.G., Baker, J., Sorden, S.D. (2018). Eye and associated glands. In A.W. Suttie (Ed.) *Boorman's Pathology of the Rat*. (Second Edition). Reference and Atlas (pp. 251-278). Academic Press
<https://doi.org/10.1016/B978-0-12-391448-4.00016-2>
PMCID:PMC7148627
2. Santillo, A., Chieffi Baccari, G., Minucci, S., Falvo, S., Venditti, M., Di Matteo, L. (2020). The Harderian gland: endocrine function and hormonal control. *Gen Comp Endocrinol.* 297, 113548.
<https://doi.org/10.1016/j.ygcen.2020.113548>
PMid:32679156
3. Bejdic, P., Avdic, R., Amidzic, L., Cutahija, V., Tandir, F., Hadziomerovic, N. (2014). Developmental changes of lymphoid tissue in the harderian gland of laying hens. *Mac Vet Rev.* 37(1): 83-88.
<https://doi.org/10.14432/j.macvetrev.2014.02.009>
4. Deist, M.S., Lamont, S.J. (2018). What makes the Harderian gland transcriptome different from other chicken immune tissues? A gene expression comparative analysis. *Front Physiol.* 9, 492.
<https://doi.org/10.3389/fphys.2018.00492>
PMid:29867543 PMCID:PMC5952037
5. Khayoon, E.S., Reshag, A.F., Almayahi, M.S., Al-Saffar, F.J. (2019). Age related changes in the cellular population and lymphoid tissue in the harderian gland of turkey. *EAJBS* 11(2): 23-32.
<https://doi.org/10.21608/eajbsd.2019.56517>
6. Hanniche, N., Saadi-Brenkia, O., Maciejewski-Duval, A., Lounis, S., Bougrid, A., Bendjelloul, M. (2019). Structural study and expression of the androgen receptors during the reproductive cycle in the harderian gland of the male *Meriones libycus*. *C R Biol.* 342(1-2): 27-34.
<https://doi.org/10.1016/j.crvi.2018.11.002>
PMid:30792115
7. Rodriguez, C., Kotler, M., Antolin, I., Sainz, R.M., Menendez-Pelaez, A. (1996). Regulation of the aminolevulinic synthase gene in the Syrian hamster Harderian gland: changes during development and circadian rhythm and role of some hormones. *Microsc Res Tech.* 34(1): 65-70.
[https://doi.org/10.1002/\(SICI\)1097-0029\(19960501\)34:1<65::AID-JEMT9>3.0.CO;2-V](https://doi.org/10.1002/(SICI)1097-0029(19960501)34:1<65::AID-JEMT9>3.0.CO;2-V)
8. EL-Leithy, E., El-Sakhawy, M.A., Al-Sabaa, A., El-Habak, H., Shaheen, Y. (2015). Seasonal immunohistochemical expression of androgen receptor (AR) in the harderian gland (HG) of male rabbit. *IJAR.* 3(8): 479-489.
9. Tatsuo, S. (1992). Comparative anatomy of mammalian Harderian glands. In S.M. Webb, R.A. Hoffman, M.L. Puig-Domingo, R.J. Reiter (Eds.), *Harderian glands: porphyrin metabolism, behavioral, and endocrine effects* (pp. 7-23). Berlin: Springer Verlag
https://doi.org/10.1007/978-3-642-76685-5_2
10. Hittmair, K.M., Tichy, A., Nell, B. (2014). Ultrasonography of the Harderian gland in the rabbit, guinea pig, and chinchilla. *Vet Ophthalmol.* 17(3): 175-183.
<https://doi.org/10.1111/vop.12063>
PMid:23738702 PMCID:PMC7169276
11. Eltony, S.A.M. (2009). A comparative study of the Harderian gland in the female rat and female rabbit (a histological, histochemical, scanning electron microscopic and morphometric study). *Egypt J Histol.* 32(1): 46-65.
12. Elgayar, S.A.M., Abou-Elghait, A.T., Sayed, A.A. (2015). Morphology of female guinea pig Harderian gland during postnatal development - secretory endpieces. *Eur J Anat.* 19(1): 15-26.
13. Lopez, J.M., Carbajo-Perez, E., Fernandez-Suarez, A., Alvarez-Uria, M. (1996). Postnatal development of cell types in the hamster harderian gland. *Microsc Res Tech.* 34(1): 48-54.
[https://doi.org/10.1002/\(SICI\)1097-0029\(19960501\)34:1<48::AID-JEMT7>3.0.CO;2-S](https://doi.org/10.1002/(SICI)1097-0029(19960501)34:1<48::AID-JEMT7>3.0.CO;2-S)
14. Bayraktaroglu, A.G., Ergun, E. (2010). Histomorphology of the Harderian gland in the Angora rabbit. *Anat Histol Embryol.* 39(6): 494-502.
<https://doi.org/10.1111/j.1439-0264.2010.01020.x>
PMid:20624156
15. Shirama, K., Ozawa, S., Seyama, Y., Kobayashi, M., Sawamura, S., Yamada, J. (1997). Postnatal development of the harderian gland in the rabbit: light and electron microscopic observations. *Microsc Res Tech.* 37(5-6): 572-582.
[https://doi.org/10.1002/\(SICI\)1097-0029\(19970601\)37:5/6<572::AID-JEMT17>3.0.CO;2-N](https://doi.org/10.1002/(SICI)1097-0029(19970601)37:5/6<572::AID-JEMT17>3.0.CO;2-N)
16. Butler, J.M., Ruskell, G.L., Cole, D.F., Unger, W.G., Zhang, S.Q., Blank, M.A., McGregor, G.P., Bloom, S.R. (1984). Effects of VIIth (facial) nerve degeneration on vasoactive intestinal polypeptide and substance P levels in ocular and orbital tissues of the rabbit. *Exp Eye Res.* 39(4): 523-532.
[https://doi.org/10.1016/0014-4835\(84\)90052-6](https://doi.org/10.1016/0014-4835(84)90052-6)
17. Pangerl, A., Pangerl, B., Buzzell, G.R., Jones, D.J., Reiter, R.J. (1989). Characterization of β -adrenoceptors in the syrian hamster harderian gland: Sexual differences and effects of either castration of superior cervical ganglionectomy. *J Neurosci Res.* 22(4): 456-460.
<https://doi.org/10.1002/jnr.490220411>
PMid:2547980

18. Zakrevska, M.V., Tybinka, A.M. (2019). Peculiarities of microstructure of the suprarenal glands of rabbits with different types of autonomic tone. *Regul Mech Biosyst.* 10(4): 415-421.
<https://doi.org/10.15421/021962>
19. Shaffer, F., Ginsberg, J.P. (2017). An overview of heart rate variability metrics and norms. *Front Public Health* 5, 258.
<https://doi.org/10.3389/fpubh.2017.00258>
PMid:29034226 PMCid:PMC5624990
20. Baeovsky, R.M., Chernikova, A.G. (2017). Heart rate variability analysis: physiological foundations and main methods. *Cardiometry* 10, 66-76.
<https://doi.org/10.12710/cardiometry.2017.10.6676>
21. Directive 2010/63/EU of the European parliament and of the council of 22 September 2010 on the protection of animals used for scientific purposes (Text with EEA relevance), Official Journal of the European Union, L 276, 33-79.
22. Mulisch, M., Welsch, U. (2015). *Romeis - Microscopic Technique*. Berlin: Springer Spektrum [In German]
<https://doi.org/10.1007/978-3-642-55190-1>
23. Pearse, A.G.E. (1960). *Histochemistry, theoretical and applied* (ed. 2). Boston: Little, Brown & Company
24. Di Matteo, L., Baccari, G.C., Minucci, S. (1995). Effect of cholinergic secretagogue substances on the morphology of the harderian gland in the frog, *Rana esculenta*. *Comp Biochem Physiol A Physiol.* 112(1): 29-34.
[https://doi.org/10.1016/0300-9629\(95\)00095-O](https://doi.org/10.1016/0300-9629(95)00095-O)
25. Coto-Montes, A., García-Macia, M., Caballero, B., Sierra, V., Rodríguez-Colunga, M.J., Reiter, R.J., Vega-Naredo, I. (2013). Analysis of constant tissue remodeling in Syrian hamster Harderian gland: intra-tubular and inter-tubular syncytial masses. *J Anat.* 222(5): 558-569.
<https://doi.org/10.1111/joa.12040>
PMid:23496762 PMCid:PMC3633345
26. Hussein, O.A., Elgamal, D.A., Elgayar, S.A.M. (2015). Structure of the secretory cells of male and female adult guinea pigs Harderian gland. *Tissue Cell* 47(3): 323-335.
<https://doi.org/10.1016/j.tice.2015.04.006>
PMid:25960413
27. Chieffi, G., Baccari, G.C., Di Matteo, L., d'Istria, M., Minucci, S., Varriale, B. (1996). Cell biology of the Harderian gland. *Int Rev Cytol* 168, 1-80.
[https://doi.org/10.1016/S0074-7696\(08\)60882-7](https://doi.org/10.1016/S0074-7696(08)60882-7)
28. Pradidarcheep, W., Asavapongpatana, S., Mingsakul, T., Poonkhum R., Nilbu-nga, S., Somana, R. (2003). Microscopic anatomy of the orbital harderian gland in the common tree shrew (*Tupaia glis*). *J Morphol.* 255(3): 328-336.
<https://doi.org/10.1002/jmor.10066>
PMid:12520550
29. Saadi-Brenkia, O., Haniche, N., Bendjelloul, M. (2013). Light and electron microscopic studies of the *Gerbillus tarabuli* (Thomas, 1902) Harderian gland. *Zoolog Sci.* 30(1): 53-59.
<https://doi.org/10.2108/zsj.30.53>
PMid:23317366
30. Rehorek, S.J., Hillenius, W.J., Sanjur, J., Chapman, N.G. (2007). One gland, two lobes: organogenesis of the "Harderian" and "nictitans" glands of the Chinese muntjac (*Muntiacus reevesi*) and fallow deer (*Dama dama*). *Ann Anat.* 189(5): 434-446.
<https://doi.org/10.1016/j.aanat.2006.10.007>
PMid:17910397
31. Maini, S., Hartley, C. (2019). Guide to ophthalmology in rabbits. *In Practice.* 41(7): 310-320.
<https://doi.org/10.1136/inp.l4775>
32. Kleckowska-Nawrot, J., Nowaczyk, R., Gozdziwska-Harfajczuk, K., Szara, T., Olbrych, K. (2015). Histology, histochemistry and fine structure of the Harderian gland, lacrimal gland and superficial gland of the third eyelid of the European bison, *Bison bonasus bonasus* (Artiodactyla: Bovidae). *Zoologia* 32(5): 380-394.
<https://doi.org/10.1590/S1984-46702015000500007>
33. Kleckowska-Nawrot, J., Gozdziwska-Harfajczuk, K., Barszcz, K., Kowalczyk, A. (2015). Morphological studies on the harderian gland in the ostrich (*Struthio camelus domesticus*) on the embryonic and post-natal period. *Anat Histol Embryol.* 44(2): 146-156.
<https://doi.org/10.1111/ahc.12124>
PMid:24995381
34. Rajathi, S., Ramesh, G., Raja, K., Kannan, T.A., Sriram, P., Hemalatha, S. (2019). Microscopic anatomy of Harderian gland in goats. *JEZS* 7(1): 1413-1418.
35. Djeridane, Y. (1996). Comparative histological and ultrastructural studies of the Harderian gland of rodents. *Microsc Res Tech.* 34(1): 28-38.
[https://doi.org/10.1002/\(SICI\)1097-0029\(19960501\)34:1<28::AID-JEMT5>3.0.CO;2-S](https://doi.org/10.1002/(SICI)1097-0029(19960501)34:1<28::AID-JEMT5>3.0.CO;2-S)
36. Marcos, H.J.A., Affanni, J.M. (2005). Anatomy, histology, histochemistry and fine structure of the Harderian gland in the South American armadillo *Chaetophractus villosus* (Xenarthra, Mammalia). *Anat Embryol.* 209, 409-424.
<https://doi.org/10.1007/s00429-005-0457-y>
PMid:15883851

37. Kozlu, T., Bozkurt, Y.A., Altunay, H., Sari, E.K. (2010). Histological and histochemical studies on the Harderian gland of the osprey (*Pandion haliaetus*). *J Anim Vet Adv*. 9(13): 1875-1879.
<https://doi.org/10.3923/javaa.2010.1875.1879>
38. Beheiry, R.R., Ali, S.A., Aref, M., Emam H. (2020). Harderian gland of flying and non-flying birds: morphological, histological, and histochemical studies. *JOBASZ* 81, 35.
<https://doi.org/10.1186/s41936-020-00175-x>
39. Chieffi, G., Chieffi Baccari, G., Di Matteo, L., d'Istria, M., Minucci, S., Varriale, B. (1996). Cell biology of the harderian gland. *Int Rev Cytol*. 168, 1-80.
[https://doi.org/10.1016/S0074-7696\(08\)60882-7](https://doi.org/10.1016/S0074-7696(08)60882-7)
40. Coto-Montes, A., Tomás-Zapico, C., Escames, G., León, J., Tolivia, D., JosefaRodríguez-Colunga, M., Acuña-Castroviejo, D. (2003). Characterization of melatonin high-affinity binding sites in purified cell nuclei of the hamster (*Mesocricetus auratus*) Harderian gland. *JPR* 34(3): 202-207.
<https://doi.org/10.1034/j.1600-079X.2003.00029.x>
PMid:12614480
41. Garcia-Macia, M., Rubio-Gonzalez, A., de Luxán-Delgado, B., Potes, Y., Rodríguez-González, S., de Gonzalo-Calvo, D., Boga, J.A., Coto-Montes, A. (2014). Autophagic and proteolytic processes in the Harderian gland are modulated during the estrous cycle. *Histochem Cell Biol*. 141(5): 519-529.
<https://doi.org/10.1007/s00418-013-1170-1>
42. Monteforte, R., Santillo, A., Lanni, A., D'Aniello, S., Chieffi Baccari, G. (2008). Morphological and biochemical changes in the Harderian gland of hypothyroid rats. *J Exp Biol*. 211(4): 606-612.
<https://doi.org/10.1242/jeb.015115>
PMid:18245638

Please cite this article as: Tybinka A., Zakrevska M., Shchepentovska O. Morphometric and histochemical features of the Harderian gland in rabbits with different types of autonomous regulation. *Mac Vet Rev* 2022; 45 (2): 157-168.
<https://doi.org/10.2478/macvetrev-2022-0024>